

ON CHANGES IN BEE NOISE STATISTICS BEFORE THE OCCURRENCE OF SEISMIC EVENTS

A. VOLVACH¹, L. KOGAN¹, L. VOLVACH¹

¹Radio Astronomy and Geodynamics Department of Crimean Astrophysical Observatory RAS,
Katsively, RT-22 Crimea

E-mail: a.volvach@gmail.com

Received August 01, 2025

Abstract. We study the anticipatory reaction of bees preceding the earthquake that occurred at 16:28:17 on September 18, 2020 (UTC) with an epicenter 12 km south-southeast of the city of Arkalochori (Southern Crete, magnitude 5.9), at 01:17:35 February 6, 2023 with the epicenter in the area of Sehitkamil (Turkey, magnitude 7.8), as well as at 02:42:27 June 22, 2023 with the epicenter 50 km south of Sevastopol (Crimea, magnitude 4.7). Shows that statistical phenomena interpreted as precursors, in all the cases considered quite clearly “gravitate” to the moment of the onset of the corresponding earthquake. The effect of a significant increase in the concentration of statistical phenomena, considered as harbingers of an approaching earthquake, was revealed during a time interval of about one day before the start of the event. The study was made of the influence of a distant earthquake on the statistics of the noise of bees in a hive. The seismic processes influence the behavior of bees in the hive at least up to distances of the order of 1200 km from the epicenter. The effect of anticipatory reaction of bees to an upcoming remote event with a characteristic time of such a reaction of the order of several hours was found.

Key words: Bee, Earthquakes, Predict, Magnetic field, Turkey

1. INTRODUCTION

In this article, based on the methodology proposed in [1-6], we study the effect of earthquakes on the statistics of physical fields generated by complex biological objects. This problem is relevant and its solution can make it possible to create a highly sensitive method for detecting a short-term harbinger of the approach of natural disasters. In particular, this applies to the forecast of impending earthquakes.

In this work, the noise of bees created by them inside the hive is considered as the studied signal. This choice is due to the wide distribution of the honey bee, the simplicity of measurements, and the existence of a complex system of acoustic communication between individual individuals. Only in the honey bee, the ability to encode information about the distance of the flight target in the duration of a

pulsating sound signal has been experimentally confirmed, and specialized organs have been identified that perceive low-frequency acoustic and electric fields [7-8]. These factors suggest the existence of a characteristic reaction of the bee colony to any external signals that can be regarded as a potential threat. Obviously, an impending earthquake is one of such threats, and the anticipatory reaction of animals to an impending seismic event has long been known [9-14]. At the same time, it would be reasonable to assume that, in relation to bees, such a reaction is rather weak compared to the background noise associated with the normal life of the hive. Therefore, in this case, a slightly different method is required to identify variations in the statistics of acoustic noise inside the hive than the methods of spectral and correlation analysis commonly used for these purposes [15-16].

In the case under consideration, we study the anticipatory reaction of bees preceding the earthquake that occurred at 16:28:17 on September 18, 2020 (UTC) with an epicenter 12 km south-southeast of the city of Arkalochori (Southern Crete, magnitude 5.9), at 01:17:35 February 6, 2023 with the epicenter in the area of Sehitkamil (Turkey, magnitude 7.8), as well as at 02:42:27 June 22, 2023 with the epicenter 50 km south of Sevastopol (Crimea, magnitude 4.7). Note that the last of these events was taken into account taking into account the small, about 70 km, distance from the epicenter point to the “measuring device” in the form of a hive with bees, which in all cases was located in the Koktebel area on the southern coast of Crimea.

The article shows that statistical phenomena interpreted as precursors, in all the cases considered (as in [1] quite clearly “gravitate” to the moment of the onset of the corresponding earthquake. Moreover, in contrast to [2], this effect manifests itself with significantly different parameters of the algorithm used. In addition, the results obtained also apply when analyzing time intervals considered that are much longer than in [3], preceding the indicated earthquakes. As a result, the probability of the appearance of such precursors “simply random,” that is, not related to the events under consideration, turns out to be very small.

The phenomenon of a sharp increase in their concentration occurs especially strongly before a very earthquake with a magnitude of 7.8 (February 6, 2023, Eastern Turkey). This fact, which is fully consistent with the methodology used, with its further verification for other similar events may turn out to be very important for making their short-term forecasts.

2. MATERIALS AND METHODS

As in [11-13], we introduce the assumption that any fields generated by bees inside the hive can be written in the following form:

$$x(t) = x_1(t) + x_2(t). \quad (1)$$

Here, the random variable (RV) $x_1(t)$ is the stochastic background noise corresponding to the normal functioning of the system, and the random process $x_2(t)$ is the response to changing external conditions. The main hypothesis put forward in this paper is the assumption of the statistical independence of these two RV.

In further calculations, we will divide the rather long, about two days, considered time intervals into a set of a large number of local segments of the implementation of the random process (Eq. 1). For any such segment, the range of values of the random process $x(t)$ is divided into N intervals with the same width h :

$$x_{min} + mh \leq x < x_{min} + (m + 1)h, \quad 0 \leq m \leq N - 1. \quad (Eq. 2)$$

The x_{min} value in (2) is different for each specified segment. Then under the condition

$$x_2(t) \neq 0 \quad (Eq. 3)$$

on the corresponding segment of the implementation with a high probability there will be a transition of part of the values of the process $x(t)$, which would take place in the case of the identical equality $x(t) = x_1(t)$, which is equivalent to the validity of the relation

$$x_2(t) = 0 \quad (Eq. 4)$$

on this entire segment, at least into neighboring cells of the form (Eq. 2), see Fig. 1.

Let us select in (Eq. 2) the width h of the sampling interval so that it would be much smaller than the effective value of the width of the distribution of values $x_1(t)$. In addition, we require the value of h to be sufficient to fall into any of the cells of partition (Eq. 2) corresponding to a significant part of the background noise range $x_1(t)$, a large number of values of this random process. As a result, with further averaging over the segments of the implementation, in neighboring cells (Eq. 2) with a high probability there may be on average an approximately equal number of process values $x(t)$. (Similar leveling, meaning a decrease in the magnitude of small local fluctuations of the corresponding empirical probability density of the measured random variable (RV) $x = x_1 + x_2$, as it is easy to understand, can be considered as an indicator of an increase in the level of chaos of processes in the system under consideration).

Thus, when (Eq. 3) is performed, as a result of the indicated transition, a significant change in the difference in the number of values in neighboring intervals (Eq. 2) will occur. Therefore, taking into account the performed calculations, we introduce into consideration a functional of the form

$$L(n) = \frac{A}{M} \sum_{l=n-M+1}^n |\mathcal{L}_l|. \quad (Eq. 5)$$

Here

$$\mathcal{L}_l = \sum_{m=0}^{N-1} (-1)^m P_{m,l},$$

where l – number of the implementation segment, m – interval number (Eq. 2), the value N is also defined in (Eq. 2), the coefficient A is introduced in order to move to the range of values of this functional that is convenient for analysis, and the argument n corresponds to the moment of completion of the implementation segment with this number. The coefficients $P_{m,l}$ are the probabilities of falling into intervals of the form (Eq. 2) when replacing, similarly to [1], the directly measured random variable $x = x(t)$ with the values of a nonlinear function of the form $\mathcal{F}[x(t)] = \sin[x(t)]$. As follows from the calculations performed, when (Eq. 3) is fulfilled, including taking into account the expected general increase in the chaotization of the processes under study, the probability of the appearance of extrema of the functional (Eq. 5) can significantly increase (which in turn will serve as a sign of a significant probability of the occurrence of the process $x_2(t)$). In further calculations, this hypothesis, which in the context of this article is equivalent to the assumption about the "condensation" of such extrema near the moments of the onset of seismic events, will be subjected to empirical verification.

3. CARRYING OUT MEASUREMENTS AND PARAMETERS OF NUMERICAL CALCULATIONS

As mentioned in the Introduction, in further calculations, the noise of bees created by them inside the hive is considered as a signal containing a possible response to seismic processes. Figures 2–4, 5–7 and 8–10 refer to the time periods before the above earthquakes on the island of Crete on September 18, 2020, in Turkey on February 6, 2023, and, respectively, south of Crimea on June 22, 2023. To demonstrate the high-probability effect of a significant difference the degree of concentration of statistical phenomena interpreted as seismic precursors in the last day before the corresponding earthquakes compared with the same period of time after their completion, in Fig. 2b, in addition to Fig. 2a, an interval of about a day after the indicated Cretan earthquake is considered. In this case, the same ones are used as for Fig. 2a, parameters of the functional $L(n)$. Taking into account such an "aftershock" interval was carried out in order to demonstrate the phenomenon of gradual attenuation of the influence of seismic processes during the period of their relaxation on the statistics of the noise of bees in the hive.

In Fig. 5, 6a and 7 consider a period of about 80 hours before the catastrophic earthquake in eastern Turkey on February 6, 2023. At the same time, in Fig. 6b is studied (with the same parameters of the algorithm used as in Fig. 6a), the time interval is about five days before the events in Turkey and, accordingly, near Crimea). Taking into account such a longer period than in the case of Fig. 6a, the interval before the indicated earthquake is carried out in order to confirm the following from the analysis of Fig. 6a of the effect of a sharp increase in the concentration of precursors as the event approaches (with the fact that, as can be seen from a comparison of Figs. 6a and 6b, the absolute majority of precursors correspond to a time interval of about 80 hours before the indicated exclusively powerful earthquake).

At the same time, in Fig. 8–10, the time period under study is also about five days before the start of an earthquake of magnitude 4.7. Such intervals were chosen to demonstrate the overall small number of precursors before the relatively weak seismic event that followed at the end of this period.

Comparison of the analysis results in Fig. 2–10 allows us to estimate the degree of increase in the concentration of precursors in the last day before the onset of the specified seismic events. In addition, considering shorter time periods in Fig. 2a, 3, 4, 5 and 6a allows us to more clearly demonstrate the properties of a set of quasi-linear structures that arise in the last few days before an approaching seismic event. In Fig. 7, 8 and 9, this kind of clarity is associated with a general relatively small number of channels and sliding boundaries that appear at the corresponding “almost quiet” time interval before the approaching relatively weak event. In Fig. 2a, 3, 4, 5, 6a, 7, 8 and 9, the time intervals from the moment of registration of the precursor to the beginning of the earthquake are indicated by thick green horizontal segments. At the same time, in Fig. 2b and 6b, similar intervals associated with the study of “additional” (compared to other figures) time periods are marked with similar blue segments. All other time intervals from the moment of registration of precursors to the beginning of the earthquake in Fig. 2b and 6b coincide with those marked in Fig. 2a and 6a.

Table 1 shows the values (in hours) of time intervals from the moment of registration of the indicated precursors and until the time of the beginning of the corresponding earthquake, corresponding to Fig. 2–10. In this case, the values of these intervals associated with taking into account additional” (compared to Fig. 2a, 3, 4, 5, 6a, 7, 8 and 9a) time intervals are marked either as “Post” (for Fig. 2b) or “Prev” (for Fig. 6b). As stated above, in all three cases the measurements were carried out in the Koktebel region on the southern coast of Crimea. The SONY ISD-PX 370 digital voice recorder was placed directly in the hive, always in the same place. To protect the device from direct contact with bees, a shell was used in the

form of a single layer of thin polyethylene. In almost all cases, continuous recording was carried out over a quasi-daily time interval of the order of 39–42 hours (as long as the battery charge was enough). When processing the data, one sample was selected from each interval of one second, corresponding to the middle of the corresponding time interval. Next, the overall ensemble of received data was divided into local implementation segments with the same number of samples in each. Then, for any such implementation segment, a statistical functional of the form (Eq.5) was calculated for $M = 100$ and $A = 1000$.

In order to analyze changes in bee noise statistics, the definitions previously introduced in (Volvach et al., 2022a) are used: local trends, testing, sliding boundaries, channels. These terms are illustrated by the example of Fig. 2a, which shows the dependence of the functional $L(n)$ at $h=0.1$, $M=300$ and the number of readings $N_1 = 120$ in any segment of the implementation. Here and below, the abscissa shows the values in minutes at $n \geq M = 100 \text{ min}$, which are counted from the moment the recorder is turned on. The red vertical solid line corresponds to the time of the beginning of the considered earthquake.

We will refer to local trends as segments of the dependence $L(n)$ located between such points of extrema of this curve for which the horizontal distance Δn from the nearest point of the curve $L(n)$ satisfies the condition.

$$\Delta n \geq 2 h. \quad (\text{Eq. 6})$$

In addition, we believe that for any local trend, the difference δL of the values of the functional $L(n)$ (Eq. 6) at the maximum and minimum points, for each of which (6) is satisfied, the inequality

$$\delta L \geq 0.2 \Delta L_{max}. \quad (\text{Eq. 7})$$

Here ΔL_{max} is the difference between the values of the largest minimum and the smallest maximum (respectively, points A and B in Fig. 2) of the considered statistical functional from the beginning of measurements to the moment of the earthquake.

Also, for a local trend, we will consider it necessary that the geometric deviation Δs of the curve $L(n)$ from a straight line segment of length Δl connecting the boundary points of this local trend would correspond to the constraint

$$\Delta s \leq 0.1 \Delta l. \quad (\text{Eq. 8})$$

All distances on the Cartesian plane $\{n, L(n)\}$ are determined here and below provided that the horizontal coordinates are normalized to the time before the onset of the corresponding earthquake, and the vertical coordinates are normalized to the value ΔL_{max} , see (Eq.7).

An example of a local trend is section ab in Fig. 2a; it also shows the distance Δs to the point that deviates most strongly from the segment connecting points a and b . The points of the boundaries of local trends will be called *guide points*. In order to emphasize the limited number of them, in Fig. 2–10, all those guide points (except for those through which channels and/or sliding boundaries are drawn, as well as additional points) are highlighted with solid rectangular contours (red for the maxima, and blue for the minima of the $L(n)$ curve).

Thus, local trends are quite large both in terms of the magnitude of variation (condition Eq. 7) and in the degree of straightness (condition Eq. 8) segments of the $L(n)$ dependence, the boundaries of which are significantly removed horizontally from any other points of this curve (condition Eq. 6), see Fig. 2a.

Let us introduce the concept of “testing”, by which we mean either the intersection at some point of the curve $L(n)$ and the straight lines of two possible types considered below, or the passage of this straight line (regardless of the existence or absence of an intersection with $L(n)$) at a distance ΔL_t vertically from the control point with coordinates $\{n_t, L(n_t)\}$ when the condition is met

$$\frac{\Delta L_t}{\Delta L_{max}} \cdot 100\% \leq 1.1\% \quad (\text{Eq. 9})$$

A *sliding boundary* is a straight line that passes through two control points and is tested by the dependence $L(n)$ at least at one more control point that satisfies condition (Eq. 7) (we will call such points additional and highlight them in the figures with a solid ellipse). Sliding boundaries are marked in the figures by solid oblique straight lines. Examples of sliding boundaries are, in particular, straight lines 3 and 6 in Fig. 2a and line 5 in Fig. 4.

A *channel* is a set of two lines, each of which passes exactly through two control points in such a way that the angle $\Delta\alpha$ between the directions of these lines satisfies the inequality

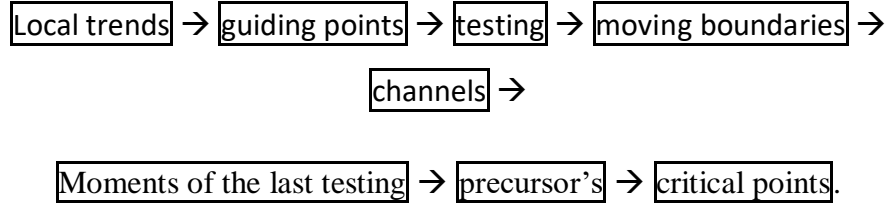
$$\Delta\alpha \leq 1.4^\circ . \quad (\text{Eq. 10})$$

In Eq. 10, the angle $\Delta\alpha$ is determined based on the properties of the scalar product of two vectors parallel to the channel boundaries, provided that the horizontal and vertical coordinates are normalized, respectively, by the value of the entire time period up to the moment of the beginning of the corresponding seismic event, and the maximum of the functional $L(n)$ in the interval before the earthquake. We believe that the time interval between the guide points through which the channel boundary is drawn is at least 150 minutes, and the lengths of such intervals for the boundaries of one channel differ by no more than three times. (We point out that a similar condition is introduced for the ratio of time intervals between two successive pairs of guide points; a sliding boundary is directly drawn through two of these

points, and the third is a guide.) In addition, the condition is introduced that at least one boundary of each channel must pass exactly either through one of the three highest maxima, or through one of the three deepest minima of the $L(n)$ curve. As an example, we point out that in Fig. 2a marked channels: 1-2, 1-3, 4-5 and 6-7. Here and below, the boundaries of the channels that do not coincide with the sliding boundaries are indicated by a dotted line.

In contrast to [1-2], as the moment of registration of a precursor of an approaching earthquake, we will consider the time of the last (before this seismic event) testing of the channel boundaries by the dependence $L(n)$ (in Fig. 2 for channels 6-7 and 1-2 by such points are respectively c and B).

Thus, the anomaly detection method consists of the following sequence of operations:



Their combination, together with very strict conditions Eq. 6 – Eq. 10, allows the use of this method.

4. CARRYING OUT CALCULATIONS

In the following Fig. 2 – 10 for all marked channels and random boundaries, conditions Eq.6 – Eq.10 are satisfied. Moreover, in most cases, the values of relations of the form Eq. 9 and Eq.10 turn out to be several times smaller than the corresponding right-hand sides of these inequalities.

On Fig. 2-4 discusses the properties of noise statistics of bees in a hive in the period before the earthquake on the island of Crete September 18, 2020.

On Fig. 2 shows the dependence of the functional $L(n)$ at the values of the parameters $h=0.1$, $M=300$ and $N_1 = 120$. Figure 2a corresponds to limited, about 10 hours, and Fig. 2b – extended, about 25 hours, time intervals after the completion of the seismic event under consideration.

In Fig. 2a the intervals $T_{2,1-2}$ (hereinafter, the first index means the number of the pattern, and the second index means the number of the corresponding time interval) correspond to the last test for sliding boundary 3 and 6, and the time

intervals $T_{2,3-7}$ correspond to the moments of the last test for channels 2–3, 4–5, 6–7, 8–9 and 1–2. (In this case, $T_{2,2} = T_{2,3} = T_{2,4} = T_{2,5}$.) In Fig. 2b all intervals $T_{2,b,1-7}$ coincide with the corresponding intervals $T_{2,a,1-7}$, while the intervals $T_{\text{Post},1} = T_{\text{Post},2}$) correspond to the time after the completion of the event. Here the interval $T_{\text{Post},1}$ is equal to the time from the last testing of sliding boundary 4, into which the lower boundary of channel 3–4 passes, see Fig. 2a, and $T_{\text{Post},2}$ is similar the period of time counted from the last testing for channel 4–11. Their physical meaning will be discussed in the Conclusions section. All values of such time intervals for Figs. 2–10 are given in the Table 1. Here and below, the control points, through which are drawn and/or which are testing points simultaneously for several channel boundaries and/or sliding boundaries, will be called critical points and marked with dotted ellipses. In Table 2 indicates the number of previously similar points before the events under consideration. On Fig. 2 there are three such points.

Table 1. Values of the intervals between the moments of registration of precursors and the start time of the corresponding earthquake.

i	$T_{2,i},$ <i>h: min</i>	$T_{3,i},$ <i>h: min</i>	$T_{4,i},$ <i>h: min</i>	$T_{5,i},$ <i>h: min</i>	$T_{6,i},$ <i>h: min</i>	$T_{7,i},$ <i>h: min</i>	$T_{8,i},$ <i>h: min</i>	$T_{9,i},$ <i>h: min</i>	$T_{10,i},$ <i>h: min</i>
1	25:01	13:0	17:23	26:06	23:56	14:23	6:56	72:12	60:4
2	16:52	4:07	1:07	19:29	22:36	14:23	1:48	25:04	31:1
3	16:52	4:07	1:07	19:29	14:49	12:54			1:46
4	16:52	2:05		11:39	10:29	12:54			1:46
5	16:52			9:41	10:23	5:42			
6	9:01			9:41	7:07				
7	5:06			9:41	4:33				
8	25:04 (Post)				68:48 (Prev)				
9	25:04 (Post)				55:44 (Prev)				
10					37:4 (Prev)				
11					28:45 (Prev)				

Table 2. The number of critical points recorded during the preparation of the corresponding seismic events.

Figure number	2a	3	4	5	6a/6b	7	8	9	10
Number of critical points	4	2	1	6	5/1	6	0	0	2

On Fig. 3 shows the dependence of the functional $L(n)$ at the values of the parameters $h=0.075$, $M=300$ and $N_1 = 120$. The interval $T_{3,2}$, corresponds to the last testing for the moving boundary 4, and the time intervals $T_{3,1}$ and $T_{3,3-4}$ correspond to the moments of the last testing for channels 1-2, 3-4, and 5-6 (point a corresponds simultaneously to the last test both for channel 3-4 and for moving boundary 4). On Fig. 3, there are two critical points.

On Fig. 4 shows the dependence of the functional $L(n)$ at the values of the parameters $h=0.1$, $M=200$ and $N_1 = 120$. The interval $T_{4,1}$ corresponds to the last test for the moving boundary 5, and the time intervals $T_{4,2}$ and $T_{4,3}$ correspond to the moments of the last test for channels 1-2 and 3-4. The moments of the last testing for both specified channels are the same, therefore $T_{4,2} = T_{4,3}$. In this case, there is one critical point.

On Fig. 5-7 discuss the properties of noise statistics of bees in a hive in the period before the earthquake on February 6, 2023 in eastern Turkey.

On Fig. 5 shows the dependence of the functional $L(n)$ at the values of the parameters $h=0.1$, $M=300$ and $N_1 = 120$. The interval $T_{5,1-2}$ and $T_{5,4}$ corresponds to the last test for sliding boundaries 3, 9 and 8, and the time intervals $T_{5,3}$ and $T_{5,5-7}$ correspond to the moments of the last test for channels 3-4, 1-2, 5-6 and 7-8. The moments of the last testing for channel 3-4 and sliding boundary 9 coincide, as well as the same moments for channels 1-2, 5-6 and 7-8. On Fig. 5 there are six critical points.

On Fig. 6 shows the dependence of the functional $L(n)$ at the values of the parameters $h=0.075$, $M=300$ and $N_1 = 120$ (similar to Fig. 3) for the case of time interval $t_0 = 80 h 26 min$ (Fig. 6a) and $t_0 = 113 h 49 min$ (Fig. 6b) the beginning of the earthquake in question. For Fig. 6a the time intervals $T_{6a,1-2}$ and $T_{6a,5-7}$ correspond to the moments of the last test for channels 3-4, 6-7, 1-2 and 4-5, and the intervals $T_{6,3-4}$ correspond to the last test for the moving boundaries 8 and 9. In this case, there is five critical points.

In Fig. 6b, blue solid thick horizontal lines mark only those T_{prev} intervals from the moment of registration of the precursor to the time of the beginning of the earthquake, which are associated with the "previous" (i.e., earlier in relation to Fig. 6a) 33-hour time interval. Here the intervals $T_{prev,1}$ correspond to the moments of the last testing for sliding boundaries 16, and the time intervals $T_{prev,2-3}$ correspond to similar moments for channels 12-13 and 14-15. In addition, in this case there is one more critical point in addition to the five such points marked in Fig. 6a.

Fig. 7 shows the dependence of the functional $L(n)$ at the values of the parameters $h=0.1$, $M=200$, $N_1 = 120$, similar to Fig. 3. The time intervals $T_{7,1}$

corresponds to the moment of the last testing for sliding limit 5, and the intervals $T_{7,2-5}$ correspond to similar times for channels 5-6, 3-4, 1-2, and 7-8. In this case, the intervals are $T_{7,1} = T_{7,2}$ and also $T_{7,3} = T_{7,4}$.

On Fig. 5-7 discuss the properties of noise statistics of bees in a hive in the period before an earthquake of magnitude 4.7 (June 22, 2023, Black Sea, 51 km south of Foros).

In Fig. 8 the functional $L(n)$ corresponds to the parameter values $h=0.1$, $M=300$, $N_1 = 120$. The intervals $T_{8,1}$ and $T_{8,2}$ correspond to the moments of the last testing for channels 3-4 and, respectively, 1-2. In Fig. 9 (здесь $h=0.075$, $M=300$, $N_1 = 120$), the intervals $T_{9,1}$ and $T_{9,2}$ correspond to the moments of the last testing for channels 1-2 and, respectively, 3-4.

In Fig. 10 (in this case $h=0.1$, $M=200$, $N_1 = 120$) intervals $T_{10,1-3}$ correspond to the moments of the last testing for channels 1-2, 3-4 and, respectively, 4-5, and the time interval $T_{10,4} = T_{10,3}$ – the interval from the moment the last testing of the sliding boundary 5 and before the start time of this earthquake. In Fig. 10 there are two critical points.

5. ANALYSIS OF THE OBTAINED RESULTS

When analyzing the results of the performed calculations, we arrive at the following conclusions.

1. For different parameters of the applied functional (Eq.5), there is a repeated occurrence of linear structures in the form of channels and sliding boundaries. This means that such phenomena are not random. Note that this article proposes a logic that boils down to proving the emergence of a set of precursors before exclusive events. “Exclusivity” in this case is understood either as the absence, during a given period of time in the region of the specified radius (counting from the hive with bees) before the earthquake in question, of events comparable to it in energy. That is, all corresponding earthquakes must have a magnitude at least one less than the given event. Or, alternatively, their epicenters must be located at least an order of magnitude further from the specified hive than the earthquake in question.

In this regard, it was taken into account that before the earthquake of magnitude 5.9 in Crete on September 18, 2020, not a single event with a magnitude of 4.9 or higher was recorded in a region with a radius of up to 5,000 kilometers for 5 days. This fact is significant, since, according to the logic of the approach used, the change in the probability density of measurements of the noise of bees in the hive will be determined precisely by the process of preparing an earthquake, which in terms of energy level far exceeds all other events expected in the corresponding region (or the epicenter of which is located close to the point of occurrence

measurements). Within the framework of a completely similar logic, the influence of the preparation process for the February 6, 2023 earthquake of magnitude 7.8 in the eastern part of Turkey was also considered. Finally, a relatively weak event of magnitude 4.7 in the Black Sea near Crimea was chosen taking into account the very short distance, about 70 km, from the beehive to the epicenter point. This approach to the selection of seismic events made it possible to demonstrate the phenomenon of concentration of precursors in the last day of preparation of the corresponding earthquakes. At the same time, it was possible to confirm not only the effect of a sharp increase in their concentration at an interval of about a day before a future event, but also, no less important, to estimate the number of such precursors corresponding to an earthquake of exclusively large magnitude.

2. Before all three considered seismic events, a set of statistical phenomena is recorded in the form of points of the last testing of channels and sliding boundaries. As follows from the Table 1, the total number of such phenomena interpreted as seismic precursors for all three applied sets of functional parameters $L(n)$ is directly proportional to the magnitude of the approaching earthquake. In relation to the 80-hour period before the corresponding event of magnitude 5.9 on September 18, 2020 (Southern Crete) it is equal to 14, and for the earthquake of February 6, 2023 with magnitude 7.8 (eastern part of Turkey) the number of such precursors is 18. Whereas for the relatively weak earthquake on June 22 2023 with a magnitude of 4.7 with an epicenter in the Black Sea near Crimea, the number of precursors is equal to 8, even when studying a significantly longer 141-hour period of time before this Crimean earthquake than for the two stronger events.

3. According to Table 1, in relation to time periods of about three and a half days, studied in Fig. 2–4, 5, 6a and 7, about half of the recorded precursors belong to the 12-hour interval before the corresponding strong earthquakes (in these figures, as well as in Fig. 6b, the durations of the corresponding time intervals are highlighted with a yellow background). Moreover, all the precursors related to these figures belong to an interval that only very slightly exceeds one day before the indicated events. This phenomenon, if further verified for other high-magnitude earthquakes, can be used for the purpose of their effective prediction. Note that all the precursors corresponding to a time interval significantly exceeding one day (i.e., starting from 30 hours and earlier before “their” earthquake), in Table 1 are highlighted with a green background.

4. Fig. 6b shows the dependence $L(n)$, corresponding to the same as in Fig. 6a, parameters $h=0.075$, $M=300$ and $N_1 = 120$, which determine the properties of this functional. This figure examines the 113-hour interval before the earthquake, which is significantly longer than the similar 80-hour period in Fig. 6a. (A larger increase in the duration of the time interval before the seismic event would not allow maintaining the clarity of the corresponding figures with a large number of channels and sliding boundaries.) A comparison of these two figures confirms the conclusion about a significant, several-fold increase in the concentration of precursors in the last

days before the approaching earthquake. Indeed, the precursors corresponding to linear objects associated with the time interval from 113 to 80 hours before a given earthquake turn out to be much more sparse in time compared to those precursors that correspond to the interval from 80 hours until the start of the seismic event, see Fig. 2a and 2b. In addition, and no less important, from a joint analysis of these figures, it follows that with the indicated increase in the duration of the time interval under study, not a single new precursor is added in a time period of about one day before the earthquake in question. The property of such an increase in the concentration of precursors of the type under consideration is typical for the statistics of measuring the noise of bees as the moments of the onset of earthquakes approach [11]. These statistical phenomena, if confirmed in relation to a number of other large-magnitude earthquakes, can be considered as signs of the approach of strong seismic events in the corresponding region of the world.

5. Fig. 2b shows a significantly larger one than in Fig. 2a, 25-hour interval after the considered earthquake in Crete. In this case, a relatively rare case was chosen when, in the period of time after the event, two simultaneously registered precursors took place. As follows from this figure, the total number of precursors during a period of about one day before and after an earthquake differs radically - even in the case when similar precursors exist after a seismic event. This fact can be interpreted as a response of the bee colony to the relaxation of seismic processes after the completion of the main phase of the earthquake. At the same time, the very fact of the emergence of the two marked in Fig. 2b "post-precursors" is connected by the existence of a linear object in the form of the lower boundary of channel 3-4, see Fig. 2a (this channel boundary later turned into a sliding boundary, see Fig. 2b), which was completely formed in the period before the earthquake. This effect can be considered as an illustration of the continuity of the influence of seismic phenomena on the population of the hive in the period both before the earthquake and during the quasi-daily interval after its completion.

6. Figures 8-10 show the dependence of $L(n)$ for an earthquake of magnitude 4.7 with an epicenter in the Black Sea near the southern part of Crimea. Here we took into account the 141-hour period before this event, which is significantly longer than in the cases of Fig. 2-4 for the event in Crete and Fig. 5, 6a and 7 for the Turkish earthquake. Despite such a long interval of the studied measurements, in the case of this Crimean event, only 8 precursors were noted in total. This number is significantly lower than for the Cretan and Turkish earthquakes. Thus, despite the longer time interval and significantly (more than an order of magnitude) shorter distance to the epicenter, the influence of the preparation processes for this Black Sea earthquake on the life activity of the hive turns out to be much less than for two other events of significantly higher magnitude. If confirmed by further research, this phenomenon can also be used in predicting high-magnitude earthquakes.

7. It should be noted that the time of registration of half (4 out of 8) of the precursors of the indicated earthquake in the Black Sea are significantly closer to the moment of its beginning to the moment of its onset (the corresponding time intervals in the last three columns of Table 1 are highlighted with a turquoise background). Indeed, as follows from Fig. 8 and 10, as well as Table 1, in this case (unlike Fig. 2–7), several times such precursors are removed from the moment of the upcoming event by no more than 2 hours. This result is consistent with the results of [11], where similar precursors for relatively weak earthquakes were also considered. This phenomenon can be explained by the fact that the preparation processes for such earthquakes with a fairly high probability exceed the noise level below which bees do not perceive them only shortly before the onset of the approaching event.

8. Figures 8–10, relating to the period before an earthquake of relatively small magnitude, can be considered as an illustration of the properties of the functional $L(n)$ in a relatively quiet period. Moreover, 7 out of 8 registered precursors are either “pressed” to the event for an interval of less than two hours, or are distant from it for a time significantly longer than one day. This situation differs significantly from the case of time periods before the other two large earthquakes considered. If such a difference is confirmed by further comparison of similar properties of statistics for other strong and relatively weak seismic events, this effect can also be applied when predicting the approach of high-magnitude earthquakes.

9. When analyzing the data in Table 2, we come to the conclusion that there is a radical difference in the total number of critical points before the Cretan (7 critical points for the 86-hour period before the event), Turkish (17 critical points for the 80-hour period before the event) and the Black Sea under consideration (total 2 critical points for the 141 hour period before the event) earthquakes. If such a difference is confirmed by the example of other seismic events of significantly different magnitudes, this phenomenon can be used to predict the approach of strong earthquakes.

10. It should be noted that the functional $L(n)$ can be considered as a characteristic of changes in the level of chaos in the measured random process [11, 14]. According to these works, the degree of this chaos turns out to be directly proportional to the magnitude of seismic compression in the area of the future hypocenter and inversely proportional to the values of the dependence $L(n)$. This article accepts the assumption discussed below that, starting from a certain level, the processes of preparation for an approaching earthquake are perceived by the population of the hive and influence its life activity. If this statement is true, the formation of channels and sliding boundaries means the emergence of barriers to the level of the corresponding chaotic influence of these processes on the behavior of bees and, consequently, on the acoustic noise generated by them.

11. In this case, the critical points discussed above with a high probability must correspond to the moments of simultaneous phenomena of the beginning, completion and/or mutual transition of both processes in preparation for the

upcoming earthquake, and the effects of a massive change in the behavior of bees inside the hive caused by them. In other words, each such point can be interpreted as a moment of simultaneous beginning or completion of several processes that affect the behavior of the bee colony and are associated with an approaching earthquake with a fairly high probability. Therefore, the phenomenon of concentration of such graphical objects over a limited period of time can also be considered as a sign of the impending significant and rapid changes in the state of the system.

12. As noted in [11], a decrease in the effective amplitude of small-scale fluctuations of the experimental probability density, which occurs under the influence of even a small but statistically independent random signal in a measured random process, is equivalent to approaching some “ideal” distribution. This distribution would correspond to an arbitrarily large number of measurements over an indefinitely long period of time. Obviously, a transition to such a distribution would mean approaching a situation of absolute chaos, that is, an unlimited growth of entropy. Thus, a decrease in the values of the functional $L(n)$, associated with a decrease in the amplitude of small-scale disturbances in the probability distribution of the signal under study with an increase in the influence of earthquake preparation processes, means an increase in the entropy of the noise of bees in the hive. Conversely, a decrease in such influence, leading to an increase in the values of $L(n)$, is associated with a decrease in the indicated entropy. Thus, the considered method of recording precursors ultimately turns out to be associated with entropy variations in the measured random process.

13. In order to further study the above assumption about the influence of the preparation processes for approaching earthquakes on the behavior of bees, two hypotheses can be put forward. The first of them boils down to exceptionally efficient mechanisms for perceiving critically important information about the phenomena of the surrounding world, developed by bees over 100 million years of evolution. The source of this kind of information can be, for example, infrasonic waves generated by faults in tectonic plates and propagating over long distances in the earth's crust in a short period of time before a seismic event and during its implementation, as well as significant variations in the electric field strength that occur during this period. The disadvantage of this assumption is the low probability of a signal passing, sufficient for perception in the measurement area, from the point of a seismic event, remote at a distance of up to 1400 kilometers. In any case, the effect of the anticipatory reaction, which takes place before the release of any significant seismic energy, is hardly explainable.

Therefore, the authors consider as an equal hypothesis the assumption of the existence of some process that is extended to large areas of space and triggers both the starting mechanism of an earthquake and the corresponding reaction from the bee colony.

6. A POSSIBLE EXPLANATION OF THE MECHANISM OF ULTRA-HIGH SENSITIVITY OF BEES TO SEISMIC PROCESSES IN THE LANGUAGE OF PROBABILITY THEORY: A MODEL OF MEDIATED PERCEPTION OF THE OBTAINED RESULTS

The results obtained require a theoretical explanation. In this section of the article, we will consider the situation from the standpoint of probability theory. Note that the anticipatory reaction of domestic animals (dogs, sheep, chickens, cows, etc.), as well as a number of reptiles and amphibians to an approaching earthquake (and this is the most interesting result in this article) has long been known. The distance at which individual animals or their small groups begin to show significant anxiety before strong events can be estimated as $\ell \sim 15 \div 30$ km from the future epicenter [13]. Let us designate as \mathcal{M} the totality of those physical phenomena to which they react.

First of all, we believe that, first of all, we should talk about the wave components of acoustic and electromagnetic fields that arise in the region near the future hypocenter immediately before the event and are weakly absorbed inside the lithosphere, as well as slightly passing into the asthenosphere. In other words, such waves propagate mainly within the boundaries of the lithosphere. Under such conditions, the decrease in the intensity of the corresponding fields at a sufficiently large distance from the hypocenter point will be linear.

According to [13], the lower limit for the probability of occurrence of an anticipatory reaction for one studied domestic animal at a specified distance from the epicenter of an impending event can be estimated as $P_0 = 0.1$. Then, at a distance of the order of $D \sim 1500$ km, the reduction factor of this quantity will be $\kappa \sim 10^{-3}$. The latter estimate takes into account the fact that the size S of the earthquake preparation zone is several tens of kilometers, and at a distance $r \lesssim S$ from the epicenter, the fields denoted as M can be considered quasi-permanent. The transition to a linear decrease in intensity is most likely for distances $r \gg S$ from the point of the emerging hypocenter. Therefore, at a distance of $\sim D$, we can consider the value κ (lower bound) to be an order of magnitude smaller than the ratio $\frac{\ell}{D} \sim 10^{-2}$ (hereinafter, we will talk about the lower bound for the value of the coefficient κ).

Thus, for any individual bee, the probability of a direct significant change in the statistics of its acoustic signals under the influence of fields generated in the area of preparation for an upcoming earthquake in the near future is estimated as $P_0 \kappa \sim 10^{-4}$ and is negligible. The value of $P_0 \kappa$ can be considered as an estimate of the proportion of changes in the acoustic parameters of the noise of an individual bee, associated with the influence of an approaching distant earthquake.

On Fig. 11 shows a typical view of the experimental histogram $f(w)$ for measurements on August 7 and 8 (Fig. 11a), September 26 and 27 (Fig. 11b) and October 4 and 5, 2019 (Fig. 11c), built with sampling interval $h_1 = 10^{-4}$. Blue curve

I corresponds to averaging over 10 consecutive values of the function $f(w)$, and red curve 2 corresponds to the theoretical Gaussian distribution for the corresponding values of the mean and variance. This figure shows that the noise of bees inside the hive does not obey the central limit theorem. Therefore, it is not a simple sum of a large number of independent random noises of individual size bees (their number in the hive was about $\mathcal{N} = 60 \div 70$ thousand individuals). Consequently, a process of continuous information exchange takes place between the bees. Its relative intensity α , defined as the share of the information component in the acoustic noise of bees, can be estimated in order of magnitude as the area of the segment under curve 1, which goes beyond the area bounded by dependence 2. As can be seen from Fig. 11, the lower limit for this value can be estimated as $\alpha \sim 20 \div 25\%$. By way of explanation, we note that the value of α determines the degree of deviation from the normal distribution. Such a deviation is possible only because of the dependence between random acoustic signals generated by individual bees, which is equivalent to the existence of information interaction between them.

Taking into account the performed calculations, the probability that, as a result of such an exchange of information between an arbitrarily chosen bee (A) and any other bee, a significant change will occur in the noise statistics of the first bee, we can estimate as $\alpha P_0 \kappa$. The probability of the reverse event is equal to $1 - \alpha P_0 \kappa$. With the independence of information influences on the bee (A) from all other bees in the hive, the total probability that its noise will not undergo significant changes associated with the approach of a distant earthquake (that is, it will not react to the corresponding slight changes in the noise of all or almost all bees in the hive) can be estimated as $(1 - \alpha P_0 \kappa)^{\mathcal{N}}$. Then for the probability P_{inf} of interest to us of the reverse event, we obtain:

$$P_{inf} = 1 - (1 - \alpha P_0 \kappa)^{\mathcal{N}} \sim 0.50. \quad (\text{Eq. 11})$$

Thus, in the case under consideration, the value of P_{inf} is statistically very significant and corresponds to the manifestation of a significant anticipatory reaction for 50% of the bees in the hive. At a greater distance, up to 5000 km, the value of κ decreases to $\sim 1.8 \cdot 10^{-4}$. In this case, by analogy with (10), the corresponding value

$$P_{inf} \sim 0.20, \quad (\text{Eq. 12})$$

which means that one-fifth of the "population" of the hive shows a significant anticipatory reaction, and so on.

Taking into account many tens of thousands of bees, relations Eq.10 and Eq.11 mean a probability close to one that at least one of the bees will eventually give an alarm signal that will spread within the hive and lead to a significant change in the noise statistics of the entire bee colony.

Now we will carry out similar calculations under the condition of decreasing the magnitude of the fields generated in the area of preparation of a seismic event, according to the law of inverse proportionality to the square of the distance. At the same time, we believe that these fields themselves are directly perceived by animals, and not their intensities (such a process can take place, for example, for the intensity of a quasi-stationary electric field). In this case, at the considered distance of ~ 1500 km, the value $\kappa \sim 10^{-5}$, and the estimate for the probability P_{inf} gives

$$P_{inf} \sim 10^{-3} \div 10^{-2}. \quad (\text{Eq. 13})$$

Even with this small value (using the estimate for the lower bound $P_{inf} = 10^{-3}$ in the calculations), we find that inside the hive the number of bees that can significantly change their behavior, which with a high probability will mean the generation of alarm signals, will be $P_{inf} \mathcal{N} \gtrsim 300 \div 500$. In other words, within the framework of the validity of the above reasoning, the discovered effect of the reaction (including the anticipatory reaction) of a bee colony to seismic events can manifest itself on very significant geographical scales.

Note also that, according to Fig. 11 about a fifth of the noise of bees is reduced to information exchange between them. In the framework of a rough estimate, this is equivalent to the fact that in a hive population of 80,000 individuals, at least 16,000 insects are engaged only in information exchange. We will assume that out of 1 mm³ of the brain of a bee, about 1% of its volume is associated with the reception and processing of information that occurs during such an exchange. Then we get that the total volume of the brain of all those bees that are involved in this information process, associated with such processing, is about 160 mm³. This value is comparable to a significant part of the processor capacity of a modern computer. With the validity of this conclusion, the ability of the bee colony to manifest an anticipatory reaction before the start of an earthquake becomes quite understandable.

As a result, we come to the assumption that a possible explanation of the detected effect of the reaction, including the anticipatory reaction, of bees to an impending earthquake can be associated with the phenomenon of collective information exchange for individuals included in the bee colony. This leads to a high probability of a significant change in the behavior of any individual bee and a change in the parameters of its noise, which causes a corresponding change in the acoustic statistics of the entire noise of the hive as a whole. The effectiveness of this kind of "collective processing of information" about potentially threatening phenomena is due to the extremely high, about 60 - 70 or more thousand individuals, the number of bees in a single hive. Thus, the bee hive radically outnumbers any other communities of biological objects available for observation both in terms of numbers and density of information exchange.

**7. POSSIBLE EXPLANATION OF THE MECHANISM OF ULTRAHIGH SENSITIVITY OF
BEES TO SEISMIC PROCESSES IN THE LANGUAGE OF PROBABILITY THEORY:
DIRECT PERCEPTION MODEL4**

In the previous section of the article, a model of mediated perception by a bee colony of information about the preparation of a distant seismic event was considered. The main mechanism of the process here was the supposed effect of the “alarming” reaction of individuals to very small changes in the statistics of noise generated by all bees inside the hive and caused by the influence of fields that occur in the preparation zone of a remote epicenter. This section discusses a possible mechanism for the occurrence of an anticipatory reaction based on the direct perception of the fields generated in the zone of preparation for an impending event by a single bee.

As follows, in particular, from [16], the amplitude of the magnetic field variations that arise in the preparation zone of a strong tectonic event and are fixed at a large, on the order of $r_1 \sim 10^4$ km, distance from it, can be a value of the order of $B_1 \sim 1 \div 2$ nT. The earthquake considered in [17] took place on March 19, 2009 in the area of the Tonga Islands, as well as in Nepal, starting from April 25, 2015. Gravimagnetic disturbances were recorded by the instruments of the North Caucasian Geophysical Observatory and, accordingly, by magnetic variometers in the village of. Karpogory, Arkhangelsk region. We believe that this kind of magnetic disturbances are created by currents flowing in the zone of preparation for an impending earthquake. Then, based on the Biot-Savart-Laplace law, we obtain that at a sufficiently large (compared to the diameter of the event preparation zone) distance R from the point of the future epicenter, the modulus B of the magnetic induction vector, also filtered over the interval of periods (Eq.13), changes according to the law

$$B \sim \frac{B_0}{R^2} . \quad (\text{Eq. 14})$$

Therefore, at the distances $r_2 \sim 10^3$ km considered above, for which the properties of the extrema of the statistical functional (Eq. 5) were studied, the corresponding amplitude values B_2 should increase in proportion to the ratio $\left(\frac{r_1}{r_2}\right)^2$, which leads to an estimate of the order

$$B_2 \sim 100 \div 200 \text{ nT} \quad (\text{Eq. 15})$$

According to [20], the minimum magnetic field variations recorded by bees are $\Delta B = 26$ nT, which is an order of magnitude less than estimate (Eq. 15). Of course, the interval (Eq. 15) refers to much stronger earthquakes than those considered in this article, with magnitude $\mathcal{M} = 7 \div 8$. At the same time, since $B_2 \gg \Delta B$, and also taking into account the considered effect of “collective processing” of

incoming information by the bee family, the possibility of a leading reaction of bees to the approaching events of a smaller magnitude is quite conceivable.

The authors would like to emphasize that the calculations carried out in this work show precisely the possibility of the existence of fairly simple mechanisms for the reaction of bees, including a leading reaction, to the approach of the onset of even very distant seismic events. These calculations should be regarded as illustrations of the main results of this article obtained earlier in Sections 1–3. More precise statements about the nature of these mechanisms can be obtained only after a series of appropriate geophysical and biophysical experiments.

8. CONCLUSIONS

In this article, a study was made of the influence of a distant earthquake on the statistics of the noise of bees in a hive. The effect of a significant increase in the concentration of statistical phenomena, considered as harbingers of an approaching earthquake, was revealed during a time interval of about one day before the start of the event. This fact means that seismic processes influence the behavior of bees in the hive, at least at distances of about 1200 km from the epicenter. The effect of a proactive reaction of bees to an upcoming distant event was discovered with a characteristic time of such a reaction from several hours to a time of the order of one day.

The article provides a possible explanation of the detected statistical phenomena. It comes down to the effect of collective processing of information by the "population" of the hive, which consists in a significant increase in the probability of a significant reaction of each individual bee to a set of very weak changes in acoustic signals emitted by all other bees. These changes are directly related to the impact of the final phase of the preparation of a strong earthquake in the region of the remote hypocenter. The mechanism of such a natural information process, which sharply increases the probability of the survival of bees as a biological species, could have arisen in the course of 100 million years of evolution. (A significant proportion of bee species live in mountain caves, crevices, and earthen burrows, and for them seismic events pose a clear threat.)

The results obtained are of a quite practical nature and allow us to raise the question of the possibility of developing a system of operational warnings about a high probability of an earthquake coming in the near future, based on acoustic noise monitoring for a sufficiently large number of bee colonies, the hives of which are separated over a long distance within a seismically hazardous region. The criterion for this high probability is reduced to a sharp increase in the number of "statistical" precursors of the species under consideration in the local time interval.

We also note that an important element of the discovered exceptionally high sensitivity of bees to the occurrence of seismic phenomena may be the place of measurements itself. This is due to the fact that in this area of the southern coast of Crimea, northern winds dominate, which blow from the steppe regions of the peninsula. They contain so little moisture that its integral content is comparable to the high-mountainous regions of the Pamirs [18]. This reduces the absorption of electromagnetic waves in the millimeter range, which, it is possible, may be carriers of the signal perceived by the bees. In addition, the place of measurements is located not so far from the ancient extinct volcano Kara-Dag. It is possible that partially preserved deep magmatic structures can serve as a channel for the propagation of low-frequency oscillations generated before an earthquake and capable of generating weak infrasonic waves perceived by biological objects upon reaching the surface. These assumptions are obviously hypothetical in nature and are subject to further verification. In particular, one of the promising directions for further research is the application of the recurrent quantitative analysis technique [18], however, not directly to the measured signal, but to the values of the $L(n)$ dependence considered in this article.

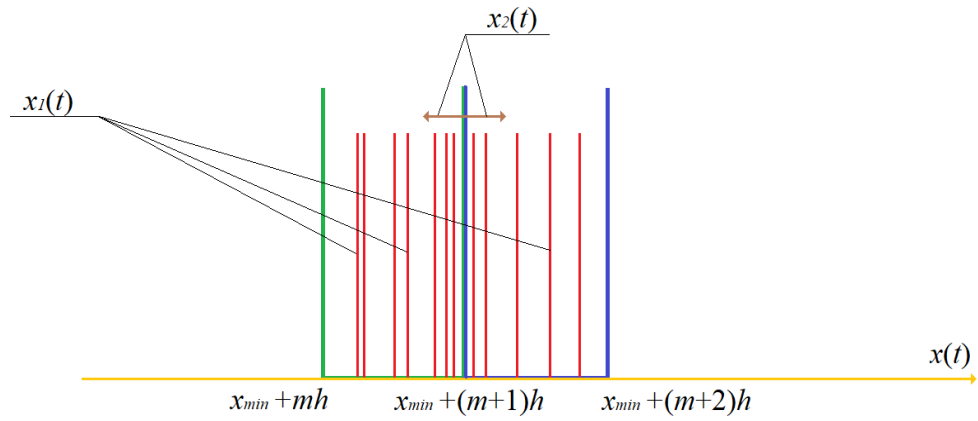


Fig. 1. The vertical red straight lines show the values of the random process $x_1(t)$ inside the cells of the form (2), and the horizontal arrows symbolically indicate the transition of the corresponding values of the $x_1(t) + x_2(t)$ to neighboring distribution cells (2) under the condition $x_2(t) \neq 0$.

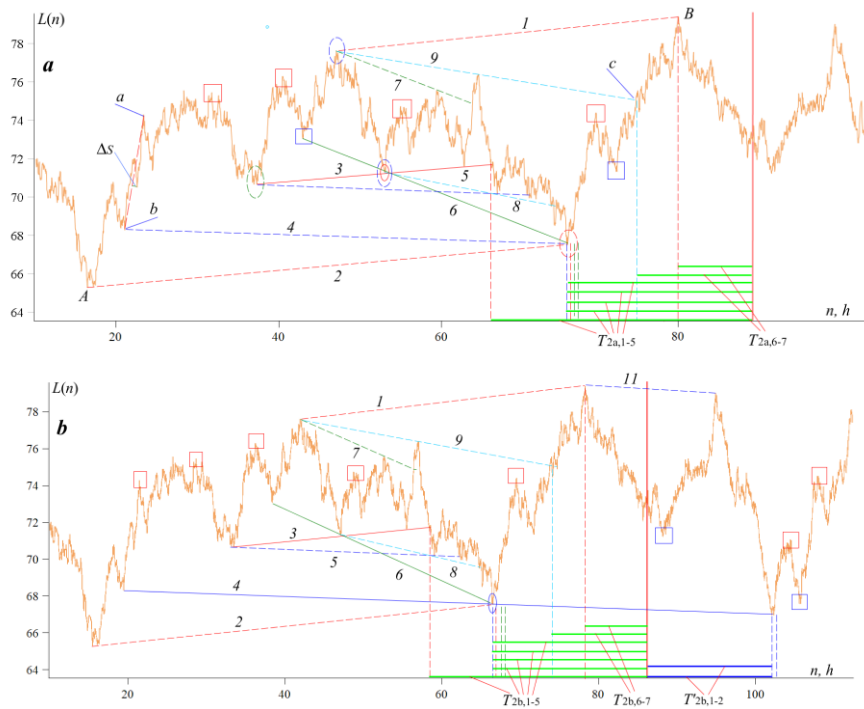


Fig. 2. $L(n)$ at $h=0.1$, $M=300$, $N_1 = 120$ for limited (a) and extended (b) time periods after the event. In addition to the time interval before the start of the considered earthquake of magnitude 5.9 (September 18, 2020), after its completion the time intervals $t_0 = 12\text{ h } 24\text{ min}$ (Fig. 2a) and $t_0 = 26\text{ h } 8\text{ min}$ (Fig. 2b) are considered. The vertical red solid line corresponds to the moment of the beginning of this event.

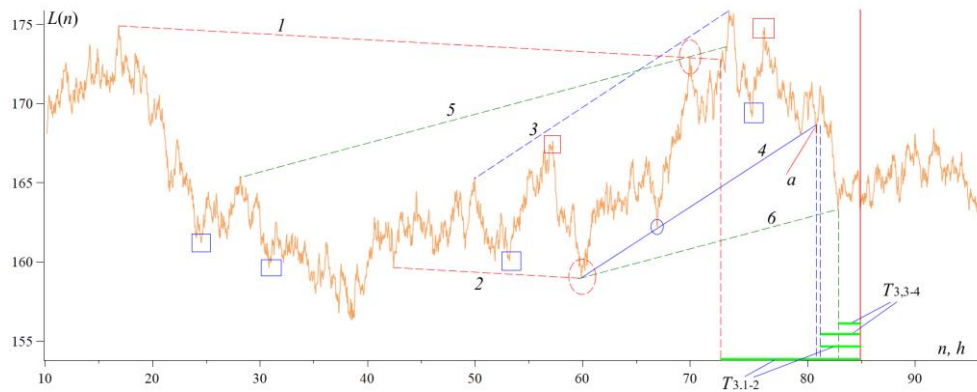


Fig. 3. Dependence $L(n)$ at $h=0.075$, $M=300$, $N_1 = 120$. The vertical red solid line corresponds to the moment of the earthquake of magnitude 5.9 (September 18, 2020).

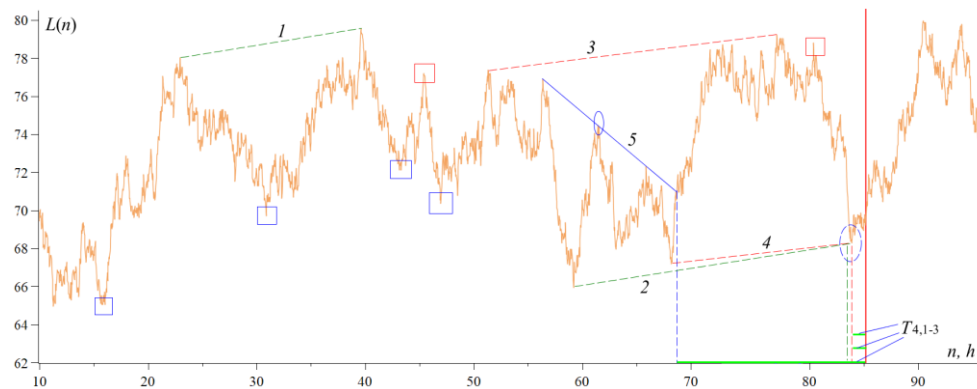


Fig. 4. Dependence $L(n)$ at $h = 0.1$, $M = 200$, $N_1 = 120$. The vertical red solid line corresponds to the moment of the earthquake of magnitude 5.9 (September 18, 2020).

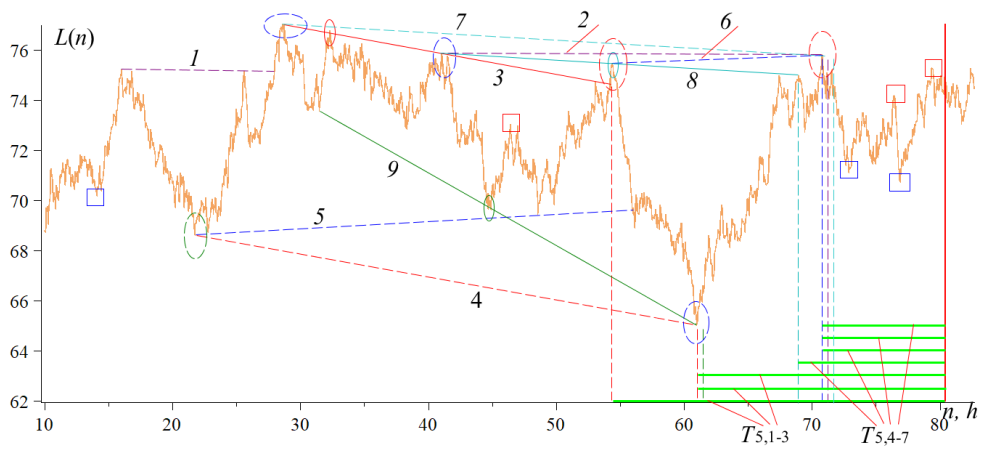


Fig. 5. Dependence $L(n)$ at $h = 0.1$, $M = 300$, $N_1 = 120$. The vertical red solid line corresponds to the moment of the earthquake of magnitude 7.8 (February 2, 2023, Turkey).

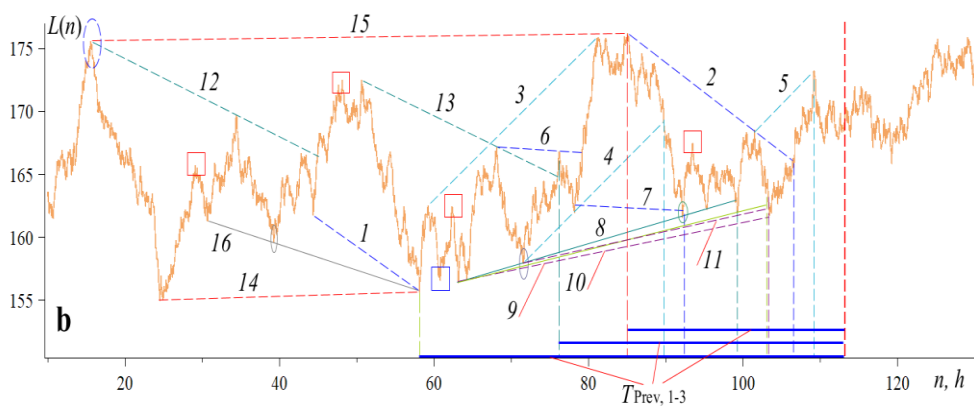
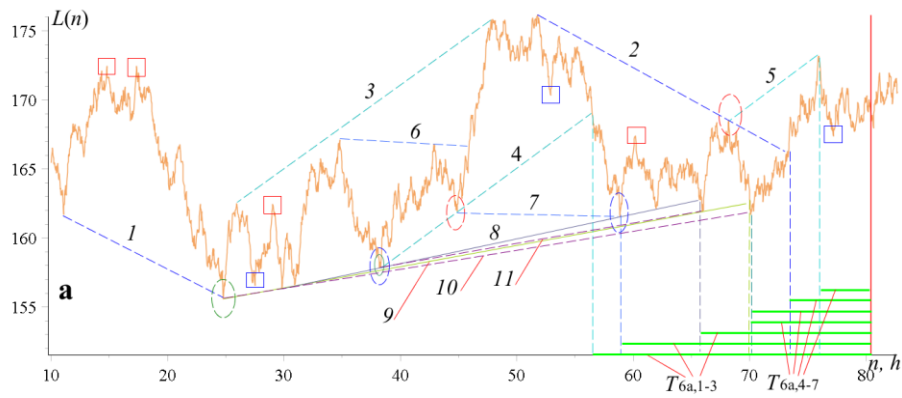


Fig. 6. Dependence $L(n)$ at $h=0.075$, $M=300$ and $N_1=120$. The time intervals $t_0 = 80\text{ h } 26\text{ min}$ (Fig. 6a) и $t_0 = 113\text{ h } 49\text{ min}$ (Fig. 6b) before the start of an earthquake of magnitude 7.8 (February 2, 2023, Turkey) are considered. The vertical red solid line corresponds to the moment of the beginning of this event.

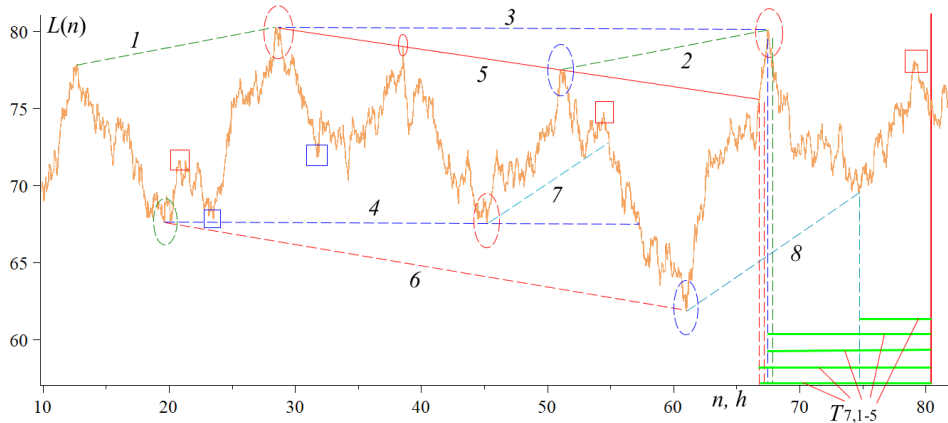


Fig. 7. Dependence $L(n)$ at $h = 0.1$, $M = 200$, $N_1 = 120$. The vertical red solid line corresponds to the moment of the earthquake of magnitude 7.8 (February 2, 2023, Turkey).

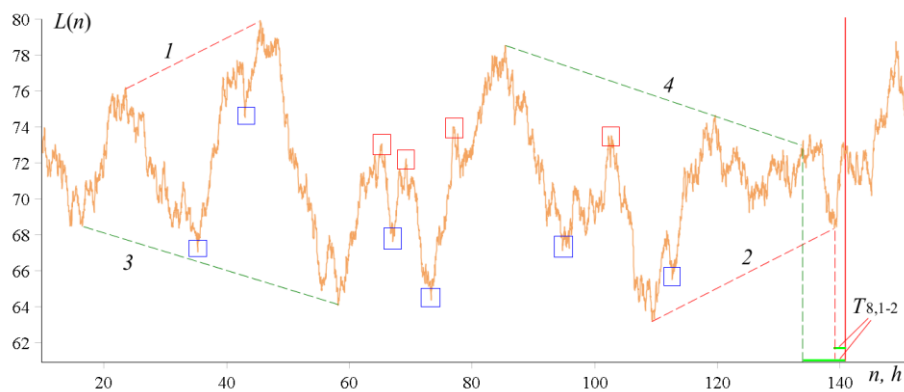


Fig. 8. Dependence $L(n)$ at $h = 0.1$, $M = 300$, $N_1 = 120$. The vertical red solid line corresponds to the moment of an earthquake of magnitude 4.7 (June 22, 2023, Black Sea, 51 km south of Foros).

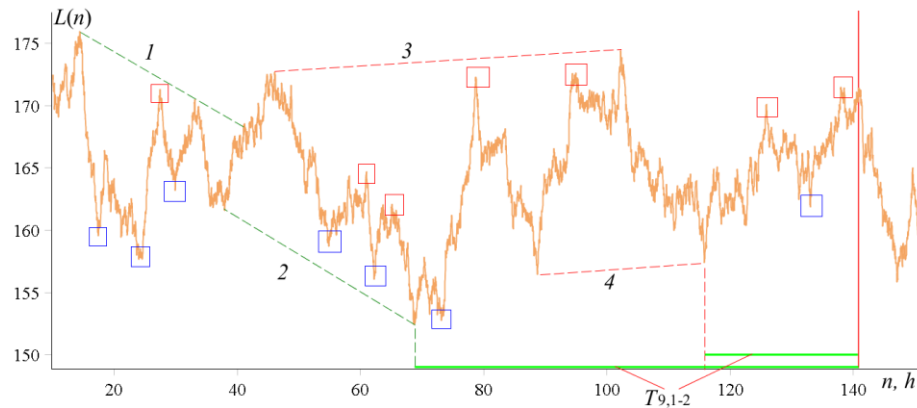


Fig. 9. Dependence $L(n)$ at $h = 0.075$, $M = 300$, $N_1 = 120$. The vertical red solid line corresponds to the moment of an earthquake of magnitude 4.7 (June 22, 2023, Black Sea, 51 km south of Foros).

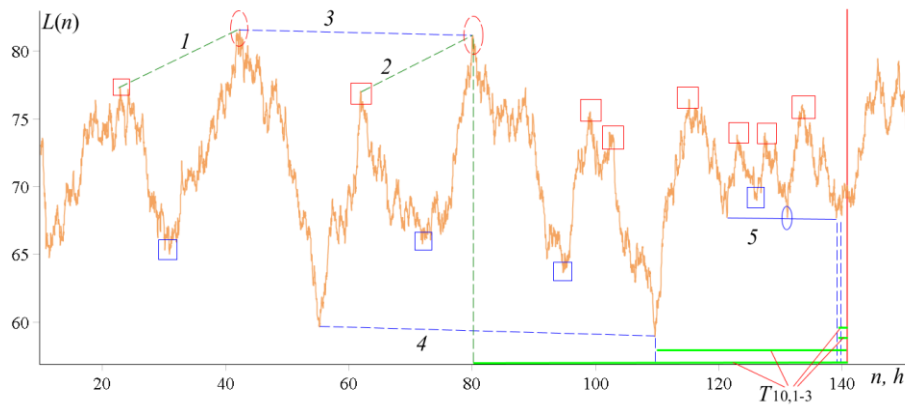


Fig. 10. Dependence $L(n)$ at $h = 0.1$, $M = 200$, $N_1 = 120$. The vertical red solid line corresponds to the moment of an earthquake of magnitude 4.7 (June 22, 2023, Black Sea, 51 km south of Foros).

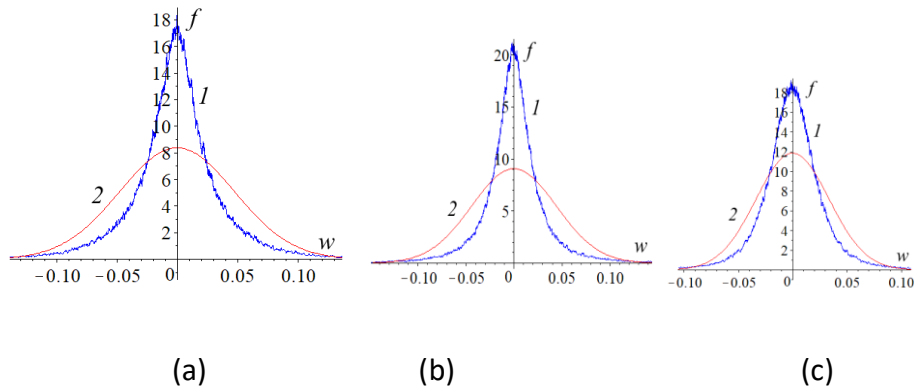


Fig.11. Experimental probability density $f(w)$.

Acknowledgment and/or disclaimers, if any

The authors express their deep gratitude to the beekeeper N.A. Kuznetsov for exceptionally significant assistance in measuring the noise of bees in the hive.

Open Research

The findings that we present in this work are reliant upon data of the noise of bees in a hive (https://drive.google.com/drive/folders/16KR-dEeH8_vRBy5shIiAWKwbmNzDIHCX?usp=sharing).

REFERENCES

1. A.Volvach, et al., Changes in the properties of the statistics of physical and biophysical fields as earthquake precursor. Communications in Nonlinear Science and Numerical Simulation 108, 106200 (2022a).
2. A. Volvach, et al., On the statistical precursors that preceded the earthquake of magnitude 6.0 on September 27, 2021, on the island of Crete. Arabian Journal of Geosciences 15, 1358 (2022b).
3. A. Volvach, et al., Statistical precursors of a strong earthquake on April 6, 2009 on the Apennine Peninsula. Heliyon 8, e10200 (2022c).
4. A.Volvach, K. Kanonidi, L. Kogan, Method for determining the probability of earthquakes based on the detection of phenomena with a high level of determinism. Official bulletin «Inventions. Utility Models». 25, Patent RU2778972C1 (2022d).
5. L. Kogan, I. Bubukin, V. Shtenberg, To the question of calculating the probability of strong earthquakes in real time. Chaos, Solitons and Fractals 145, 110807 (2021).

6. L. Kogan, Change in statistical functionals of critical frequency prior to strong earthquakes. *Geomagnetism and Aeronomy* 55(4), 507–520 (2015).
7. C. Hsu, F-Y. Ko, C. Li, et al., Magnetoreception System in Honeybees (*Apis mellifera*). *PLoS ONE* 2(4), e395 (2007).
8. E. Eskov, V. Toboev. Analysis of statistically homogeneous fragments of acoustic noises generated by insect colonies. *Biophysics* 55, 92 (2010).
9. P. Mai, et al. Monitoring pre-seismic activity changes in a domestic animal collective in Central Italy. *Geophysical Research Abstracts* 20, EGU2018-19348 (2018).
10. A. Deshcherevskii, A. Sidorin Changes in the behavior of fishes and insects before earthquakes at the Garm test site. *Doklady Earth Sciences* 399(8), 1172-1176 (2004).
11. P. Wilson, Detecting bee hive behavioral changes through frequency and signal analysis of audio files. Honors Thesis 57p. A (2019).
https://libres.uncg.edu/ir/asu/f/Wilson_Preston_August%202019_Honors%20Thesis.pdf
12. Wikelski M., et al., Potential short-term earthquake forecasting by farm animal monitoring. *Ethology* 126, 931 (2020).
13. J. Kirschvink Earthquake Prediction by Animals: Evolution and Sensory. *Perception Bulletin of the Seismological Society of America* 90(2), 312 (2000)
14. C. Fidani, Biological Anomalies around the 2009 L’Aquila Earthquake. *Animals* 3(3), 693 (2013).
15. A. Rybochkin, S. Saveliev, M. Shamsan, Analysis of acoustic noise of a bee colony. *Beekeeping* 3, 54 (2013).
16. A. Rybochkin, S. Mohsen, Diagnosing the state of bee families on produced by them acoustic noise. *Alternative Energy and Ecology* 18, 123 (2014).
17. A. Spivak, S. Riabova, Geomagnetic Variations during Strong Earthquakes. *Izvestiya-physics of the solid earth* 55(6): 811 (2019)
18. I. Bubukin, et al., *Astron Rep* 65(7), 598–614 (2021).